Studies of the Nonlinear Evolution of the $m = 1$ Sawtooth Mode in Extended MHD Models

Kai Germaschewski, Amitava Bhattacharjee

Space Science Center

University of New Hampshire

July 14, 2006

Collaborators: Luis Chacon, Chung-Sang Ng

Introduction

Reconnection in nature is often not steady.
Impulsive behavior is found in a wide variety of systems, e.g.

- sawtooth oscillations in tokamaks
- magnetotail substorms
- solar flares

Resistive MHD alone cannot explain those processes, we examine the effects of an extended Ohm's law including Hall term, electron inertia and electron pressure gradient effects.

Overview

- Introduction
- Adaptive Mesh Refinement
- 2D extended MHD
- A non-staggered, conservative, $\nabla \cdot \vec{B} = 0$ finite volume scheme for 3-D extended MHD in curvilinear coordinates
- Implicit time integration
- 3D Hall-MHD
- Conclusion

Adaptive mesh refinement

Example: 2D ideal MHD

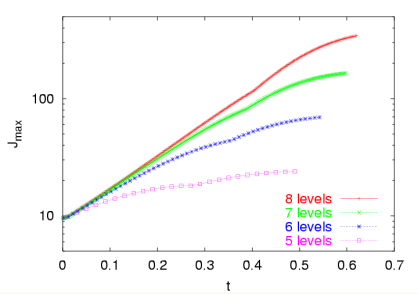

Efficiency of AMR

Level	# grids	# grid points
0	0	0
1	0	0
2	0	0
3	0	0
4	134	34304
5	295	75520
6	554	141824
7	872	223232
8	1492	382208

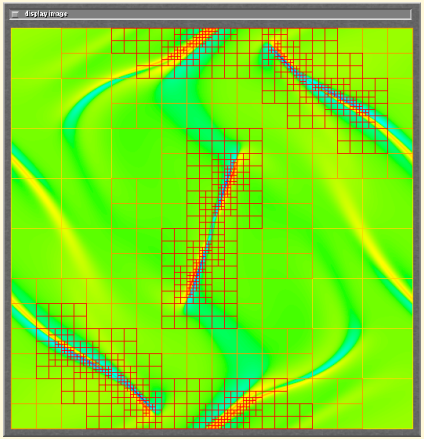

Grid points in adaptive simulation:	857088
Grid points in non-adaptive simulation:	16777216
Ratio	0.05

Load balancing

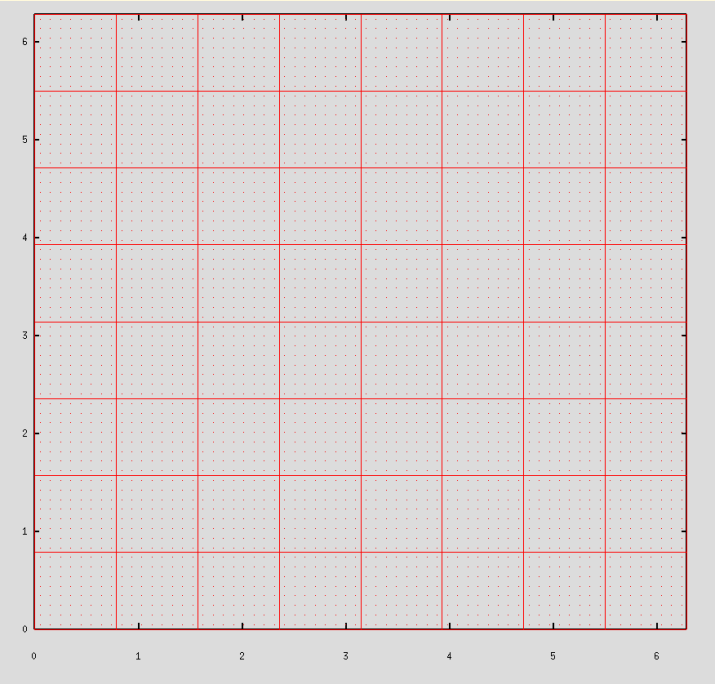

Domain $2\pi \times 2\pi$, subdivided into 8×8 grids with 8×8 grid points each.

Load balancing

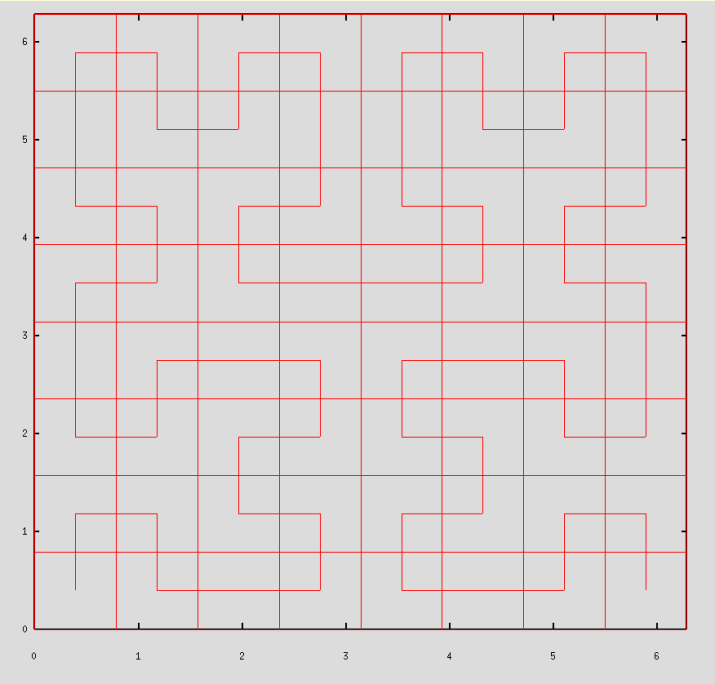

Hilbert–Peano space filling curve

Domain $2\pi \times 2\pi$, subdivided into 8×8 grids with 8×8 grid points each.

Load balancing

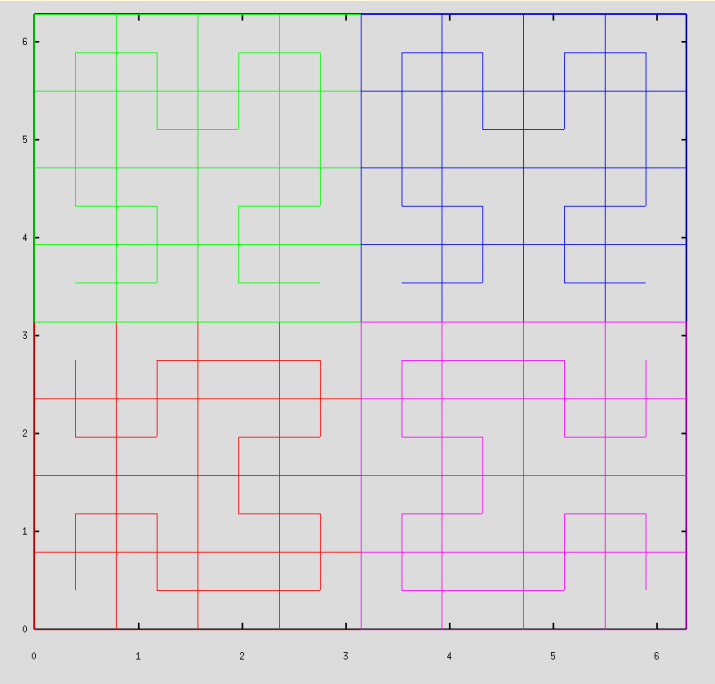

Hilbert–Peano space filling curve, distributed to 4 processors

Domain $2\pi \times 2\pi$, subdivided into 8×8 grids with 8×8 grid points each.

Load balancing

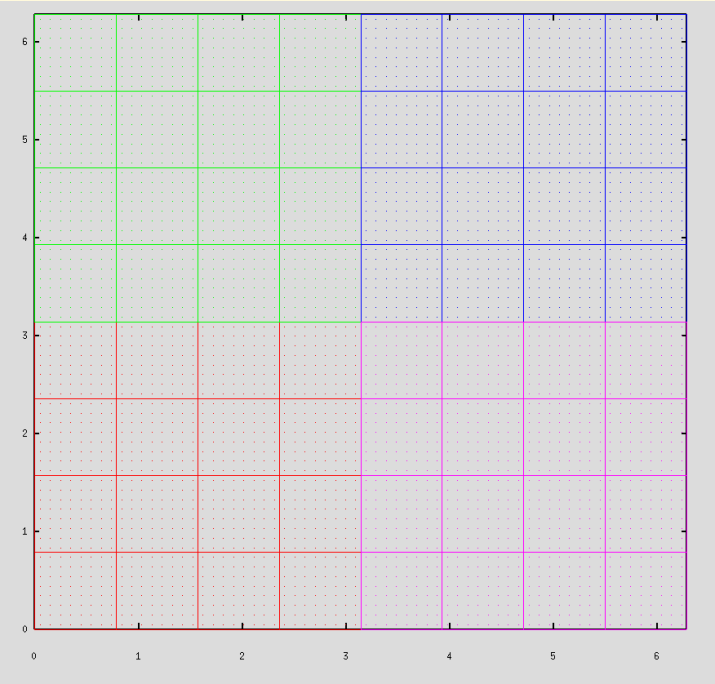

Distribution to 4 processors

Domain $2\pi \times 2\pi$, subdivided into 8×8 grids with 8×8 grid points each.

Load balancing

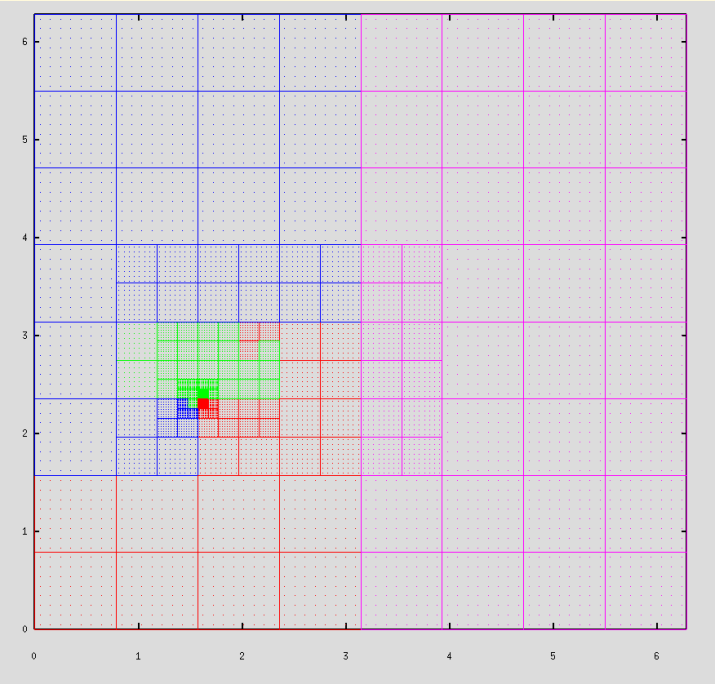

Four levels of refinement

Domain $2\pi \times 2\pi$, subdivided into 8×8 grids with 8×8 grid points each.

Load balancing

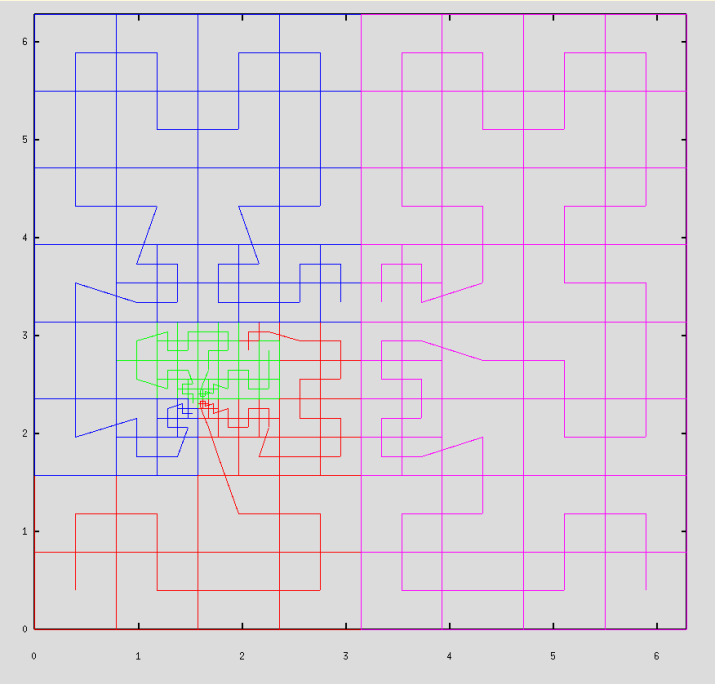

Four levels of refinement, corresponding Hilbert-Peano curve

Domain $2\pi \times 2\pi$, subdivided into 8×8 grids with 8×8 grid points each.

Discretizing Poisson's equation on an AMR hierarchy

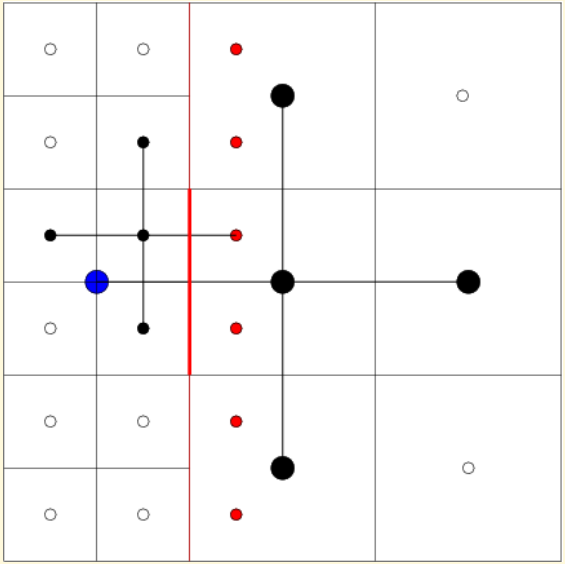

Poisson's equation:

$$\nabla^2 \vec{x} = \vec{b}$$

Remember $\nabla^2 \vec{x} = \nabla \cdot \nabla \vec{x}$
$\Longrightarrow$ treat conservatively!

Solve iteratively with multigrid / multilevel method

- scales like $O(N \log N)$ / $O(N)$, where N is the total number of grid points.

```
Solve()
{
  Calculate residual on level l_fine;
  MG(l_fine)
}

MG(l)
{
  if (l == 0)
    correction[l] = SolveCoarse(residual[l])
  else
    correction[l] = 0
    Smooth(correction[l])
    Restrict remaining residual to level l-1
    Calculate residual on unconvered grids on level l-1
    MG(l-1)
    correction[l] += Prolong(correction[l-1])
    Smooth(correction[l])

  solution[l] += correction[l]
}
```

Multilevel Poisson solver

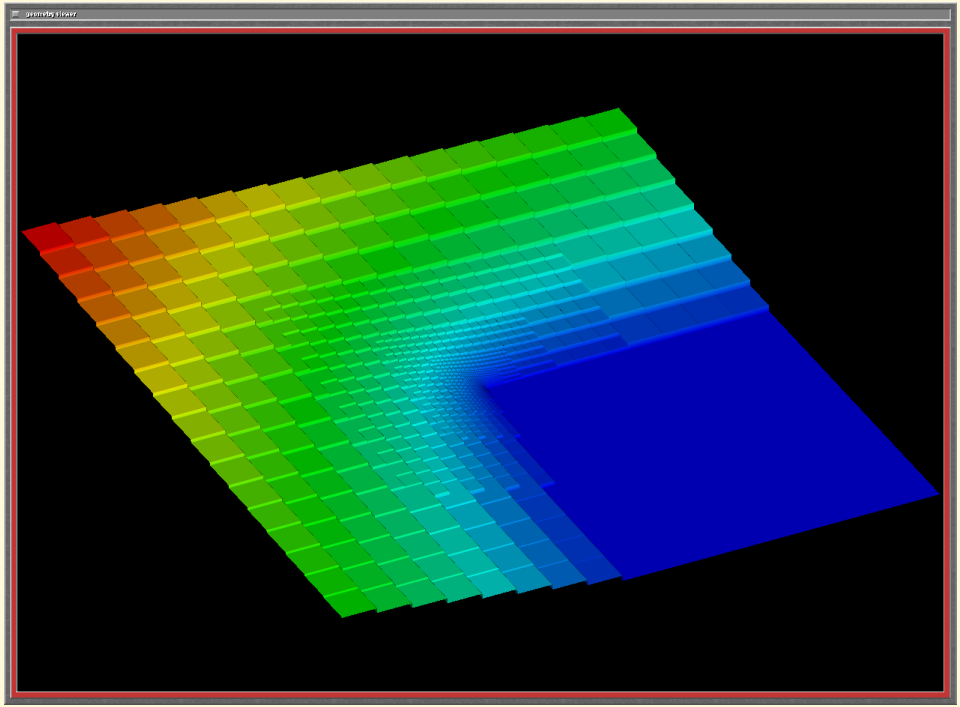

Multilevel Poisson solver – zoom

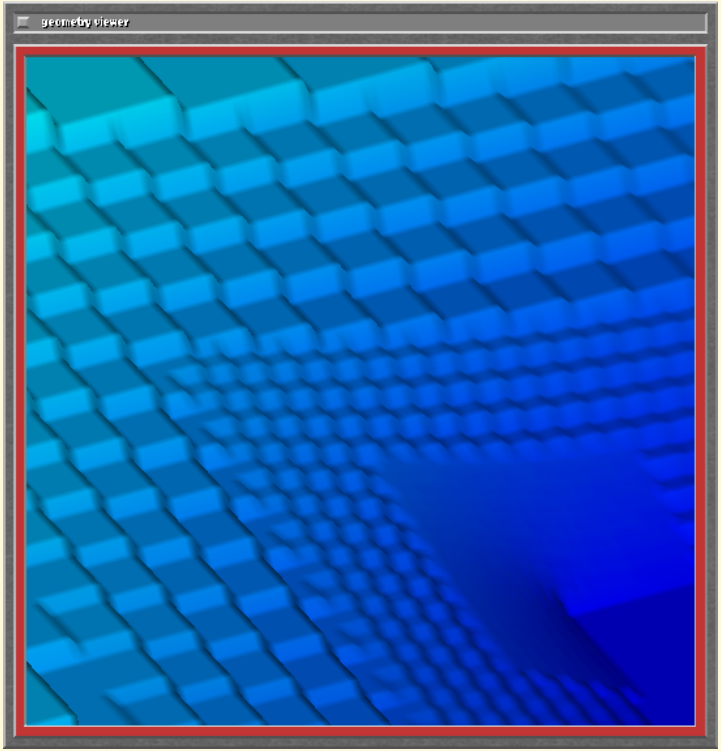

2D extended MHD

(Ottaviani/Porcelli 1993)
(Grasso/Pegoraro/Porcelli/Califano 1999)

Model equations

$$
\begin{aligned}
\partial_t F + [\phi, F] &= \rho_s^2 [U, \psi] \\
\partial_t U + [\phi, U] &= [J, \psi] \\
F &= \psi + d_e^2 J \\
J &= -\nabla^2 \psi \qquad\qquad \mathbf{B} = B_0 \hat{\mathbf{z}} + \nabla\psi \times \hat{\mathbf{z}} \\
U &= \nabla^2 \phi \qquad\qquad \mathbf{v} = \hat{\mathbf{z}} \times \nabla\phi
\end{aligned}
$$

with $[A, B] = \hat{\mathbf{z}} \cdot \nabla A \times \nabla B$.

Equilibrium

$$
\begin{aligned}
\phi_{eq} &= U_{eq} = 0 \\
\psi_{eq} &= J_{eq} = \cos(x) \quad , \quad F_{eq} = (1 + d_e^2)\cos(x)
\end{aligned}
$$

Resolving the current sheet

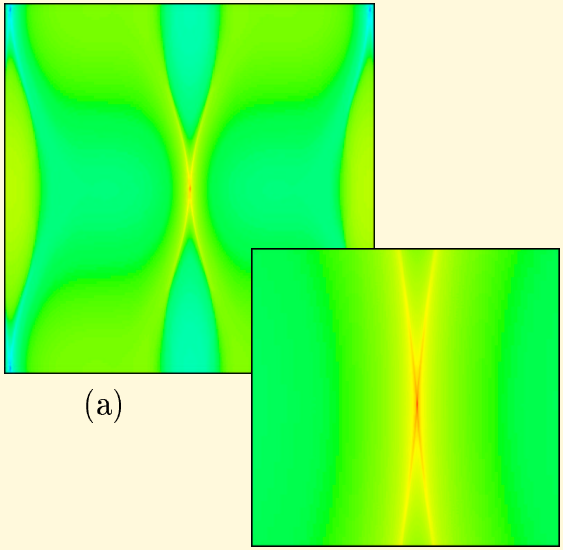

(a)

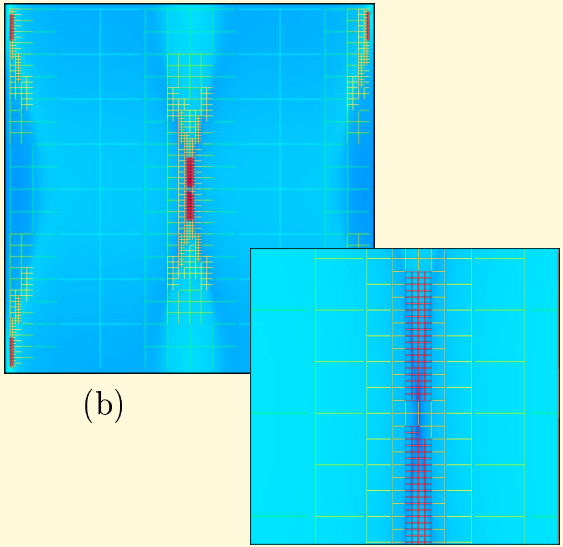

(b)

Nonlinear evolution of the tearing mode

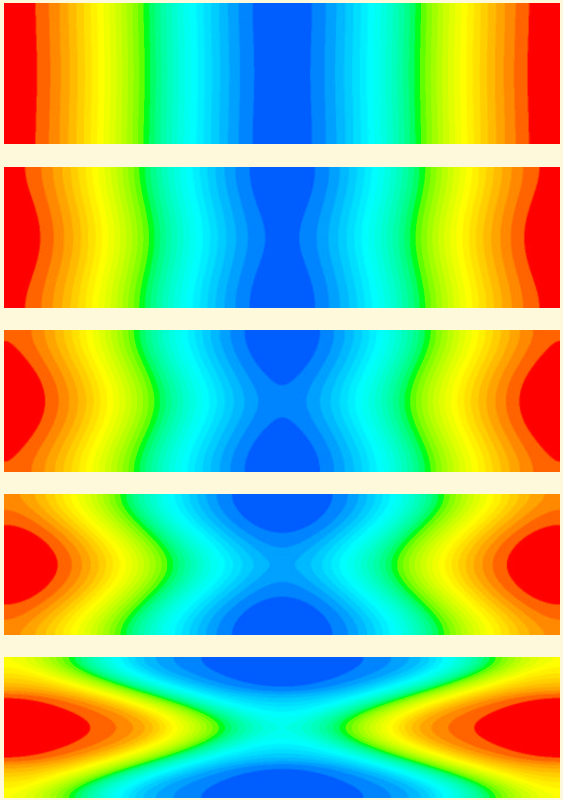

flux ψ

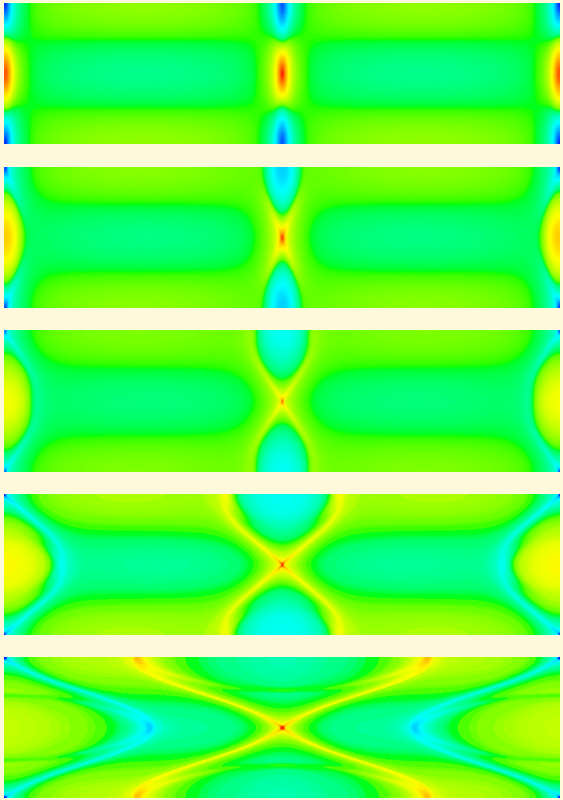

current J

Analytical model:
Analytically, an island equation for the nonlinear evolution is derived:

$$\frac{d^2\hat{w}}{d\hat{t}^2} \approx \frac{1}{4}(\hat{w} + c_J\hat{w}^4)$$

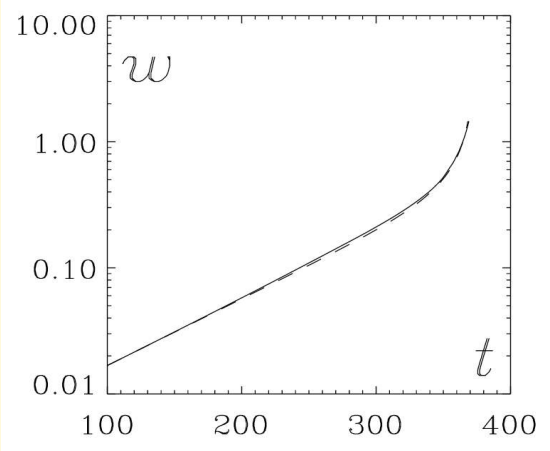

The plot shows the Island half-width $\hat{w}$ as a function of time from numerical simulation (solid curve) and from the analytic equation with $c_J = 0.1$ (dashed curve), for the case $\rho_s = 0.2$, $d_e = 0.1$, $k = 0.5$, $\gamma_L = 0.0024$.

Scaling with ρ_s

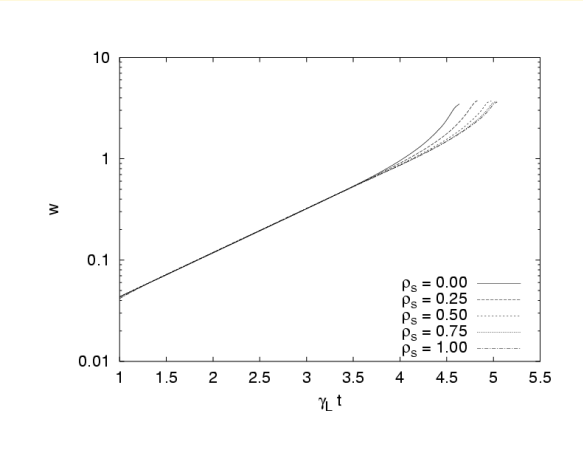

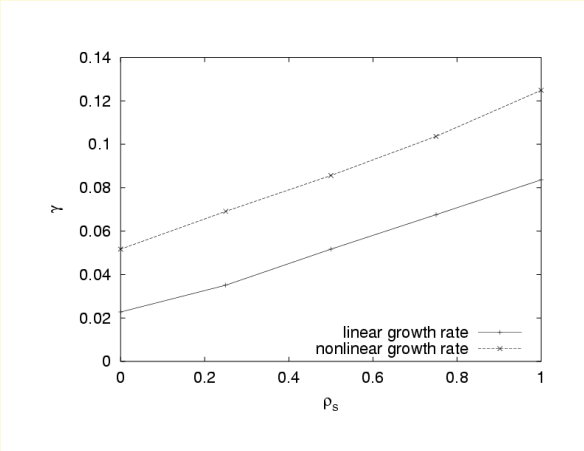

Island width time evolution for different values of ρ_s for $d_e = 0.25$, $\epsilon = 0.5$, time rescaled with linear growth rate (left), linear and nonlinear growth rates (right).

Scaling with wavenumber k

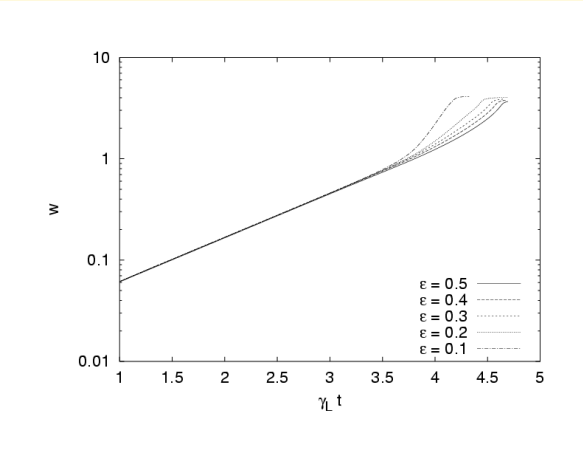

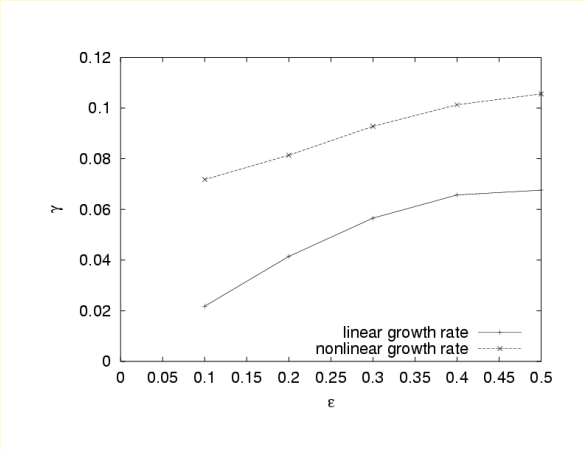

Island width time evolution for different values of ϵ $(= k)$ for $\rho_s = 0.75$, $d_e = 0.25$, time rescaled with linear growth rate (left), linear and nonlinear growth rates (right).

Four-Field Model

(Aydemir 1992)

Model equations

$$\frac{\partial U}{\partial t} + [\phi, U] + \nabla_{\parallel} J = d_i \tau \nabla_{\perp} \cdot [p, \nabla_{\perp} \phi],$$

$$\frac{\partial \psi}{\partial t} + \nabla_{\parallel}[\phi - (1+\tau) d_i p] = \eta J + d_e^2 \left(\frac{\partial J}{\partial t} + [\phi - d_i \tau p, J] \right),$$

$$\frac{\partial p}{\partial t} + [\phi, p] + \beta \nabla_{\parallel}(v + 2 d_i J) = 0,$$

$$\frac{\partial v}{\partial t} + \frac{1}{2}(1+\tau)\nabla_{\parallel} p + [\phi - d_i \tau p, v] = 0$$

$$J = \nabla_{\perp}^2, U = \nabla_{\perp}^2 \phi, \tau = T_i / T_e$$

$$\beta = \frac{nkT_e}{B_T^2 / 2\mu_0}, d_i = \frac{c/2\omega_{pi}}{a}, d_e = \frac{c/\omega_{pe}}{a}$$

Nonlinear evolution

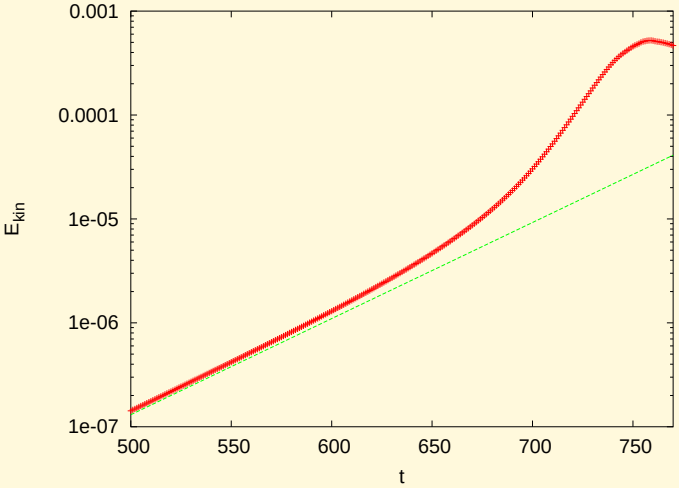

We do indeed reproduce Aydemir's results and observe an explosive growth phase in the nonlinear phase, until the finite volume inside the $q = 1$ surface of the island quenches furth growth.

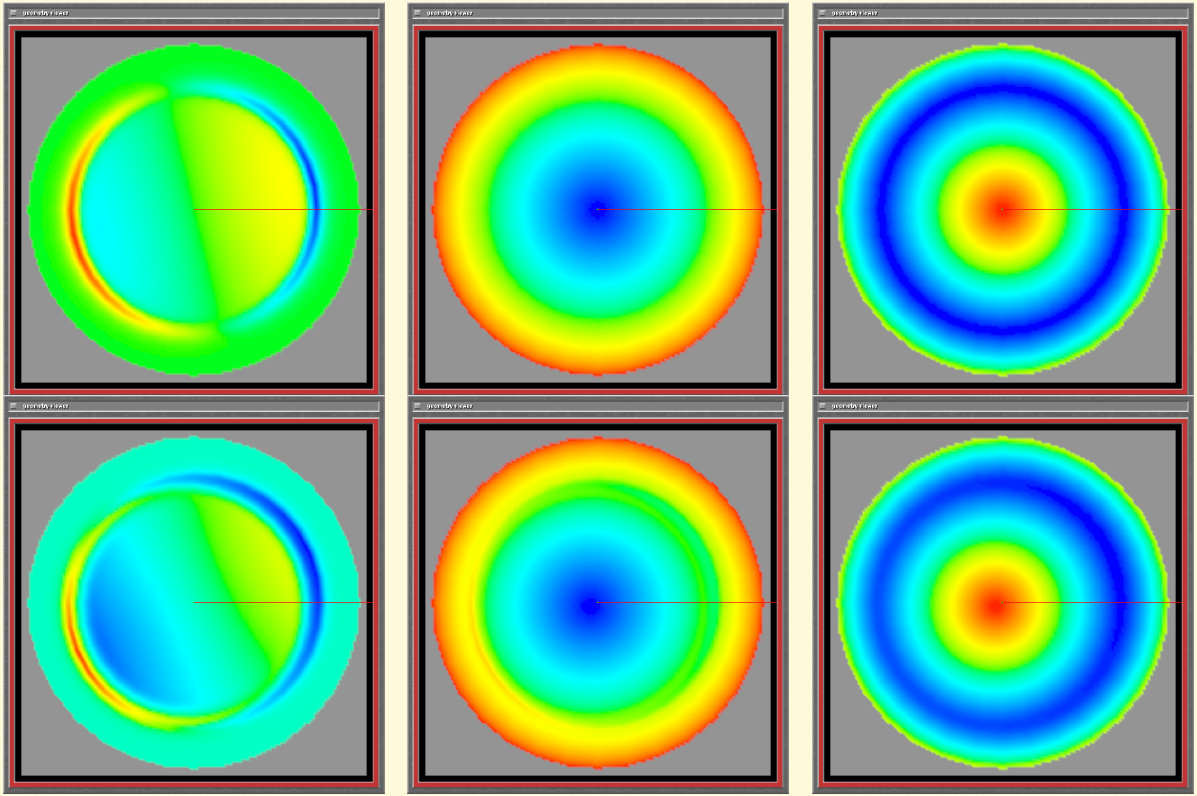

$J - J_0$ J ψ

Parameters: $d_i = 0.11$, $d_e = 0.005$, $\eta = 10^{-6}$, $\beta = .005$

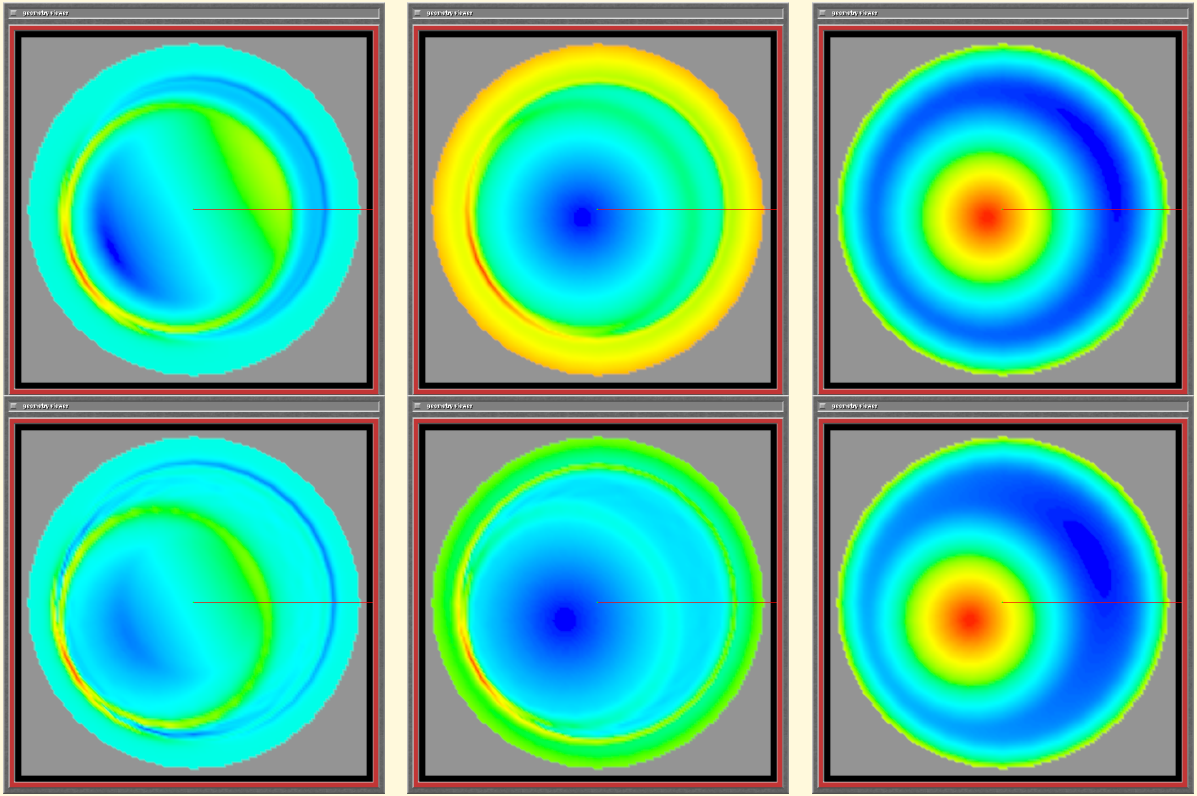

$J - J_0$ J ψ

Parameters: $d_i = 0.11$, $d_e = 0.005$, $\eta = 10^{-6}$, $\beta = .005$

3D Hall-MHD

A non-staggered, conservative, $\nabla \cdot \vec{B} = 0$ finite volume scheme for 3-D extended MHD in curvilinear coordinates (L. Chacon 2004)

Model equations

$$
\begin{aligned}
\frac{\partial \rho}{\partial t} &= -\nabla \cdot (\rho \vec{v}) \\
\frac{\partial (\rho \vec{v})}{\partial t} &= -\nabla \cdot \left[\rho \vec{v}\vec{v} - \vec{B}\vec{B} + \overleftrightarrow{I}\,(p + \frac{B^2}{2}) - \rho \nu \nabla \vec{v} \right] \\
\frac{\partial \vec{B}}{\partial t} &= -\nabla \times \vec{E} \;\; ; \quad \vec{E} = -\vec{v} \times \vec{B} + \frac{d_i}{\rho}(\vec{J} \times \vec{B} - \nabla p_e) + \eta \vec{J} \;\; ; \quad \vec{J} = \nabla \times \vec{B} \\
\frac{\partial T}{\partial t} &= -\vec{v} \cdot \nabla T - (\gamma - 1) T \nabla \cdot \vec{v}
\end{aligned}
$$

3D Hall-MHD

Given an arbitrary mapping $\vec{x} = \vec{x}(\vec{\xi})$, define contra- and convariant bases:

$$\vec{i} = \nabla \xi_i \quad , \quad \underrightarrow{i} = \frac{1}{J} \frac{\partial \vec{x}}{\partial \xi_i}$$

(and metric tensors $g^{ik} = J\vec{i} \cdot \vec{k}$, $g_{ik} = J\, \underrightarrow{i} \cdot \underrightarrow{k}$, Christoffel symbols Γ^i_{jk}, where J is the Jacobian of the transformation) Normal vectors are irrotational ($\nabla \times \vec{i} = \vec{0}$), tangential vectors are solenoidal ($\nabla \cdot \underrightarrow{i} = 0$).

$$\begin{aligned}
\partial_t(J\rho) &= -\partial_i(\rho v^i) \\
\partial_t(\rho v^i) &= -\partial_n(J^{-1}T^{ni}) + J^{-1}T^{nk}\Gamma^i_{nk} \\
\partial_t B^i &= -\epsilon_{ink}\partial_n E_k \\
\partial_t(JT) &= -v^i\partial_i T - (\gamma - 1)T\partial_i v^i
\end{aligned}$$

where $\partial_i = \partial/\partial\xi_i$, A^i, A_i contra-/covariant vector components and

$$\begin{aligned}
T^{ki} &= \rho v^k v^i - B^k B^i + g^{ki}(Jp + B_n B^n/2) - \rho\nu[\nabla\vec{v}]^{ki} \\
E_i &= J^{-1}\epsilon_{ink}v^n B^k - \eta j_i
\end{aligned}$$

3D Hall-MHD – Spatial discretization

Finite volume discretization of terms in divergence form:

$$\partial_x(\rho v)_i = \frac{(\rho v)_{i+1/2} - (\rho v)_{i-1/2}}{h}$$

where the underlying quantities are given on a cell-centered grid.
Need to interpolate the flux to faces:

- $(\rho v)_{i+1/2} = \frac{1}{2}[(\rho v)_{i+1} + (\rho v)_i]$ (flux average)
- $(\rho v)_{i+1/2} = \frac{1}{2}[\rho_i v_{i+1} + \rho_{i+1} v_i]$ (ZIP)

Both schemes are 2nd order and conservative, but ZIP additionally satisfies a numerical chain rule property and is nonlinearly stable.

Faraday's Law

Using the divergence as defined above and simple finite differences for the partial derivatives in the curl operator, this scheme preserves div B to round-off.

3D Hall-MHD – Tearing test

Cartesian grid

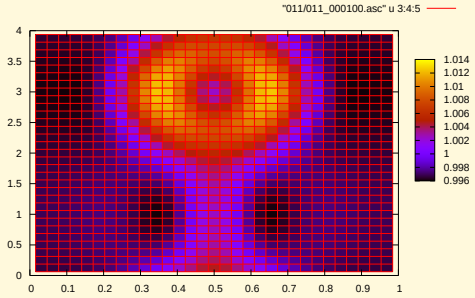

Sinusoidally distorted grid

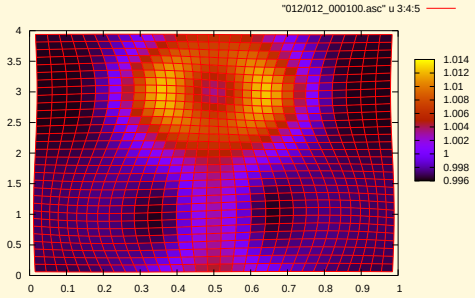

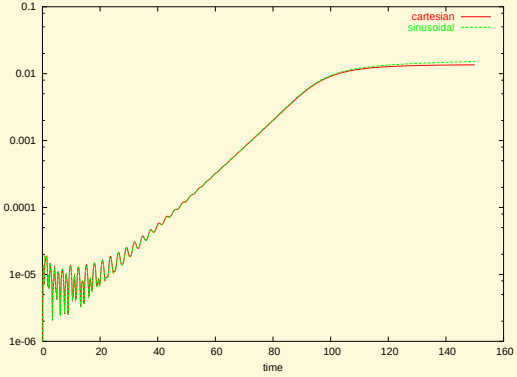

Implicit time integration

Whister waves, kinetic Alfven waves are dispersives waves, $\omega \sim k^2$

$$\Longrightarrow \Delta t_{cfl} \sim (\Delta x)^2$$

Solution: Implicit timestepping (Crank-Nicholson)

$$\partial_t \vec{x} = RHS(\vec{x}) \quad \longrightarrow \quad \frac{\vec{x}^{n+1} - \vec{x}^n}{\Delta t} = \frac{1}{2}(RHS(\vec{x}^{n+1}) + RHS(\vec{x}^n))$$

Need to solve nonlinear equation $F(\vec{x}^{n+1}; \vec{x}^n, t) = 0$.
Newton's method:

$$x_{i+1} = x_i - F(x_i)/F'(x_i)$$

generalizes straight-forward to multi-dimensions, but need to solve linear problem to invert Jacobian.
Use Krylov accelerator for the linear problem, then we only need directional derivatives which can be approximated by

$$F'(\vec{x})\vec{v} \approx \frac{F(\vec{x} + h\vec{v}) - F(\vec{x})}{h}$$

(matrix-free Newton-Krylov-Schwarz)
Implemented in PETSc library.

Implicit time integration – Direct solvers

Unfortunately, matrices are ill-conditioned for large timesteps and preconditioning is a hard problem.

Solution: Use a direct solver (SuperLU). Only re-factorize if necessary. Works well for up to medium sized problems (e.g, matrix size $2 \cdot 10^6$ squared, number of nonzero elements $3 \cdot 10^9$).

Need to actually build the sparse matrix.

Code generator

Example $\partial_t \rho = -\frac{1}{J} \partial_i (\rho u^i)$:

```
v_rU   = vector_zip(zBASE2(_RHO, _U));
t[RHO] = NEG(MUL(REC(_JAC(0,0,0)), vDIV(v_rU, 0,0,0)));
```

```
  FLD3(r,jx,jy,jz,RHO) =
(
  -((0.5*(RHO(x,jx+0,jy+0,jz+0)*
          (P0(x,jx+1,jy+0,jz+0) / RHO(x,jx+1,jy+0,jz+0)) +
          RHO(x,jx+1,jy+0,jz+0) *
          (P0(x,jx+0,jy+0,jz+0) / RHO(x,jx+0,jy+0,jz+0))) -
     0.5*(RHO(x,jx-1,jy+0,jz+0) *
          (P0(x,jx+0,jy+0,jz+0) / RHO(x,jx+0,jy+0,jz+0)) +
          RHO(x,jx+0,jy+0,jz+0) *
          (P0(x,jx-1,jy+0,jz+0) / RHO(x,jx-1,jy+0,jz+0)))) /
    (CRD0f(jx+1) - CRD0f(jx+0))
    +
...
```

Code generation

Code generator advantages:

- Calculates derivatives symbolically.
- Generates optimal code for a given coordinate transformation, non-uniform grid, set of parameters, number of dimensions, ...
- Algorithms easier to maintain / change.
- Can easily be adapted to generate code in a different programming language.

Disadvantages:

- Good simplification of symbolic expressions is difficult to implement.
- Generated code (with back-substituted boundary conditions) gets very long and complex.

Implicit time integration

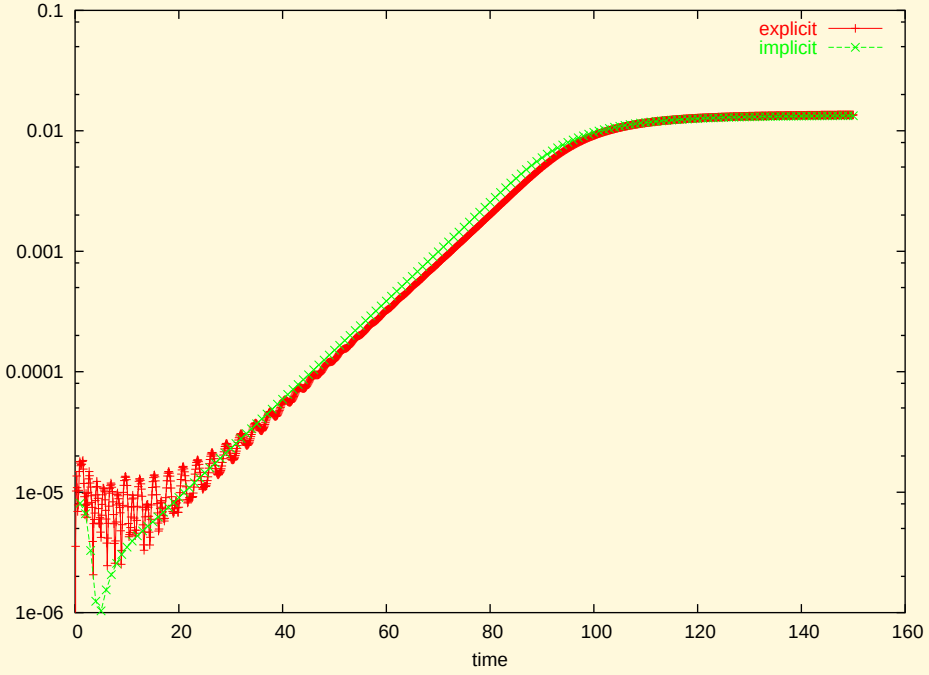

3D Hall-MHD

Model equations

$$
\begin{aligned}
\frac{\partial \rho}{\partial t} &= -\nabla \cdot (\rho \vec{v}) \\
\frac{\partial (\rho \vec{v})}{\partial t} &= -\nabla \cdot \left[\rho \vec{v}\vec{v} - \vec{B}\vec{B} + \overleftrightarrow{I}\,(p + \frac{B^2}{2}) - \rho \nu \nabla \vec{v} \right] \\
\frac{\partial \vec{B}}{\partial t} &= -\nabla \times \vec{E} \;\; ; \quad \vec{E} = -\vec{v} \times \vec{B} + \frac{d_i}{\rho}(\vec{J} \times \vec{B} - \nabla p_e) + \eta \vec{J} \;\; ; \quad \vec{J} = \nabla \times \vec{B} \\
\frac{\partial T}{\partial t} &= -\vec{v} \cdot \nabla T - (\gamma - 1) T \nabla \cdot \vec{v}
\end{aligned}
$$

Equilibrium

$$
\begin{aligned}
J_{z_0}(r) &= \frac{J_0}{[1 + (r/r_{ch})^2]^2}, \\
B_{z_0} &= 1/\epsilon
\end{aligned}
$$

The $q = 1$ surface is located at $r = 0.2$ for our choice of J_z, r_{ch}.

Verification: Linear resistive tearing mode

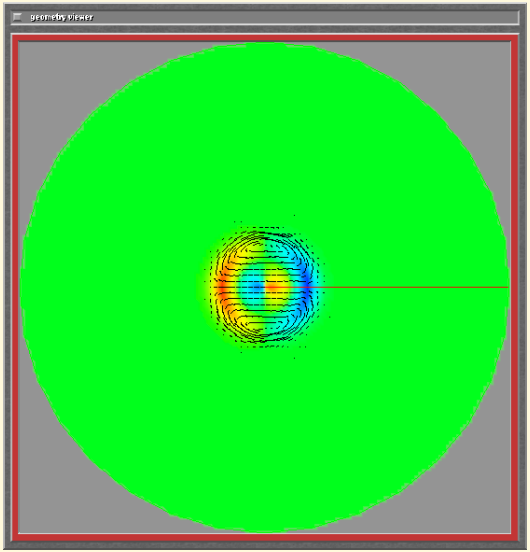

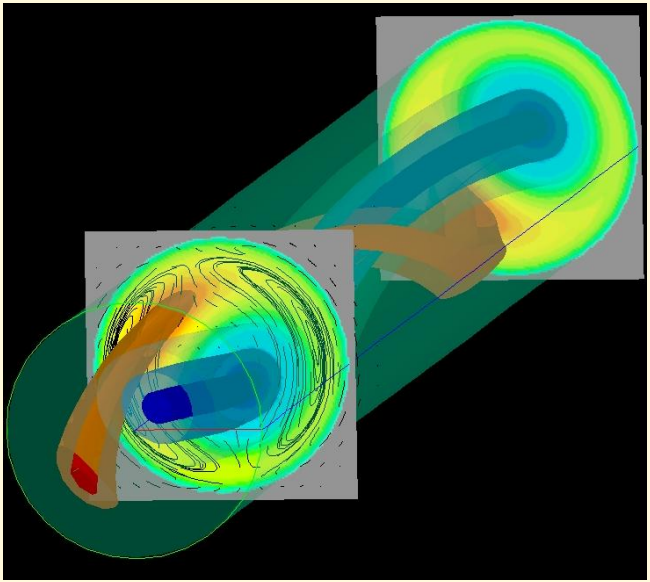

To the left, we show a plot of the poloidal magnetic field (colored) and streamlines of the in-plane plasma flows. The three-dimensional plot visualizes the m=1 cylindrical tearing mode after the island has grown to macroscopic size.

Nonlinear resistive evolution

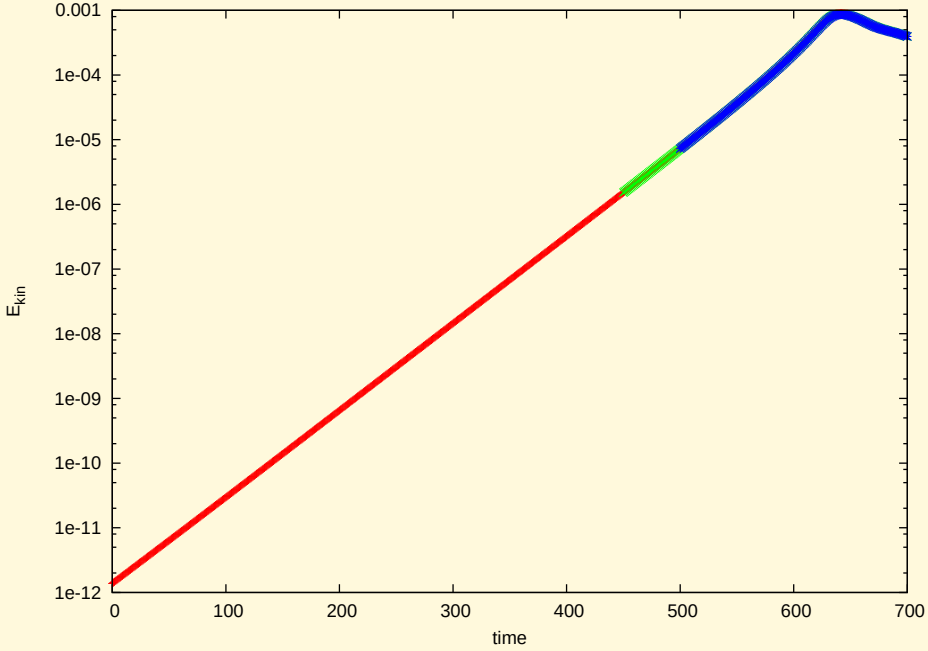

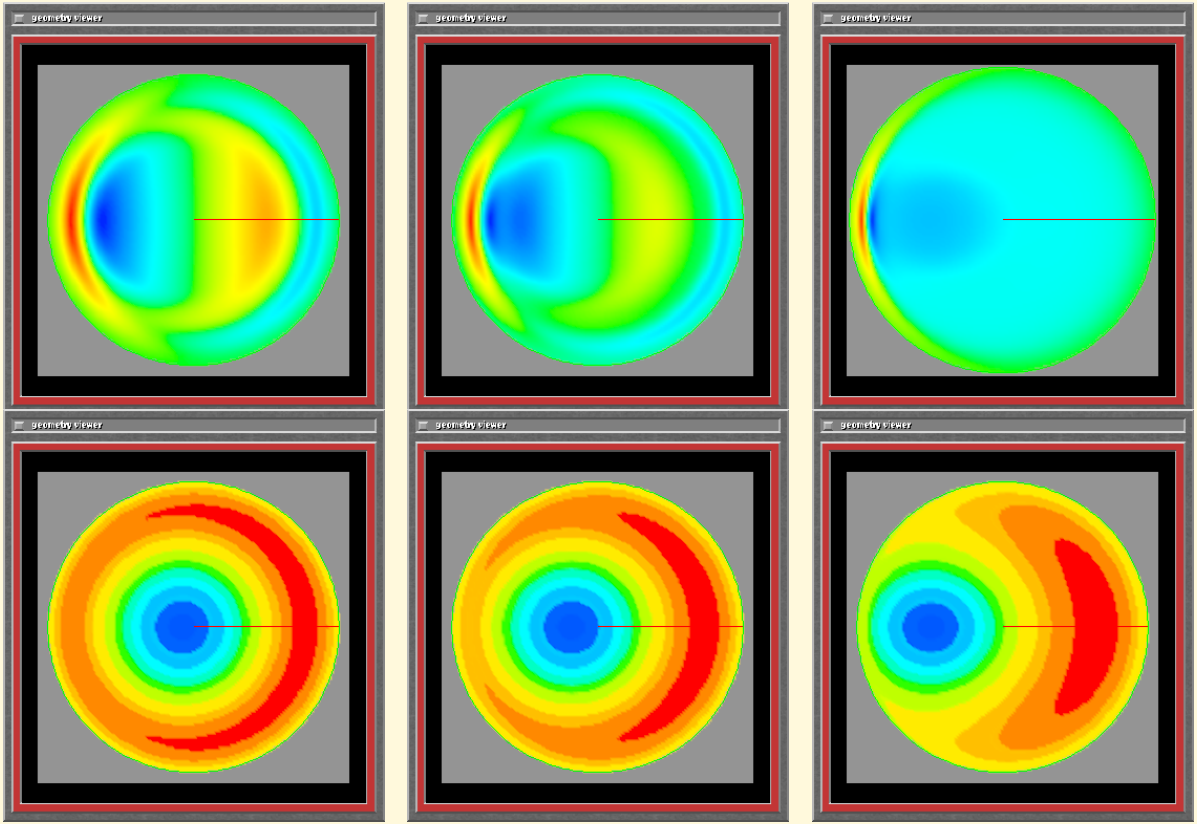

J_{pert}, ψ at $t = 500$ J_{pert}, ψ at $t = 550$ J, ψ at $t = 600$

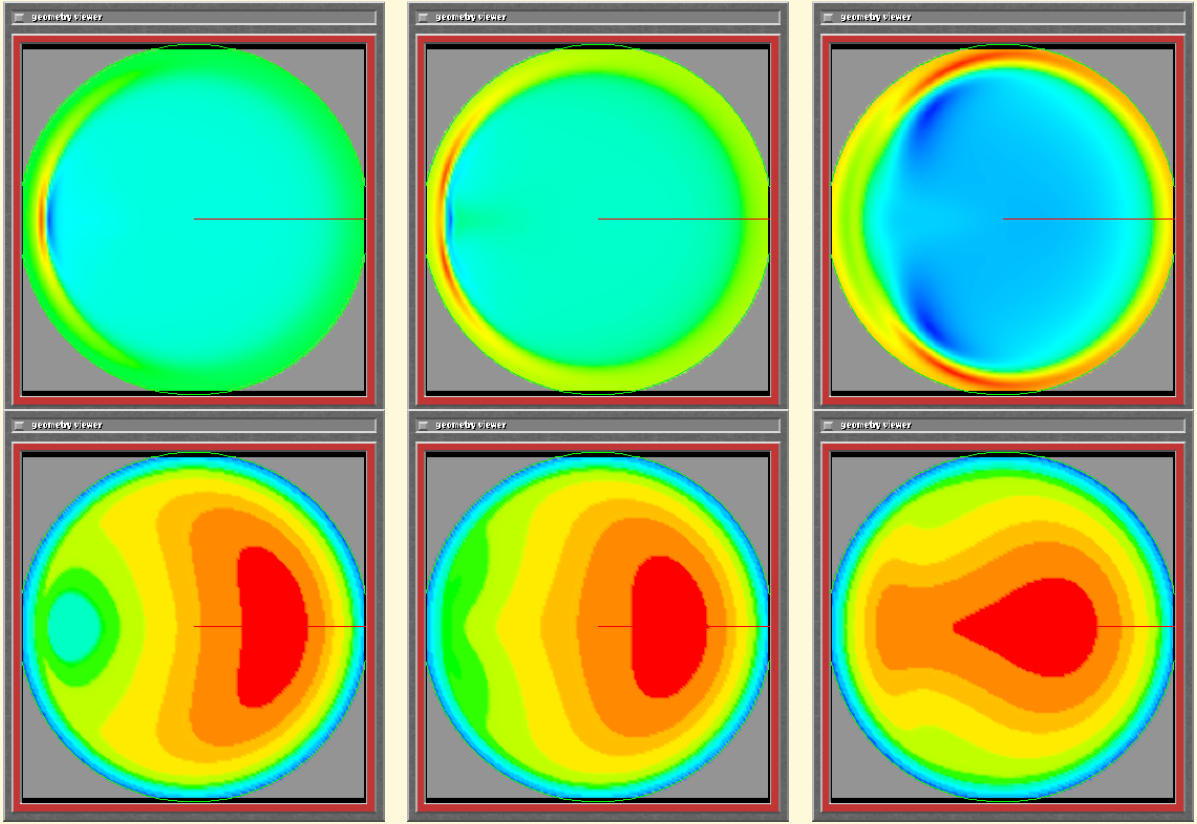

J, ψ at $t = 620$ J, ψ at $t = 630$ J, ψ at $t = 650$

Put in Hall effects: $d_i = 0.05, \eta = 10^{-6}$,
and vary aspect ratio ε:

aspect ratio ε	nonlinear behavior	γ_r	γ_i
.3	slightly accelerated	.00850	-.00188
.2	accelerated	.00929	-.00093
.1	strongly accelerated	.00835	-.00015
(four-field)	strongly accelerated	.0106	0

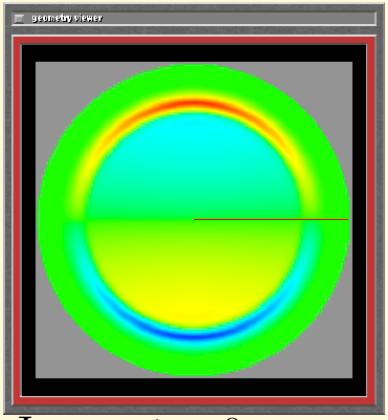

J_{pert} at $t = 0$

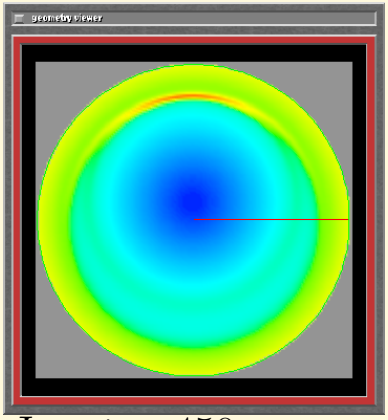

J at $t = 450$

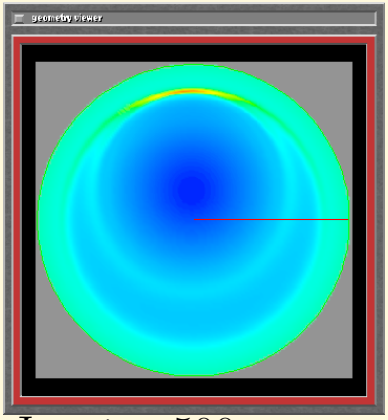

J at $t = 500$

Nonlinear Hall-MHD accelerated growth

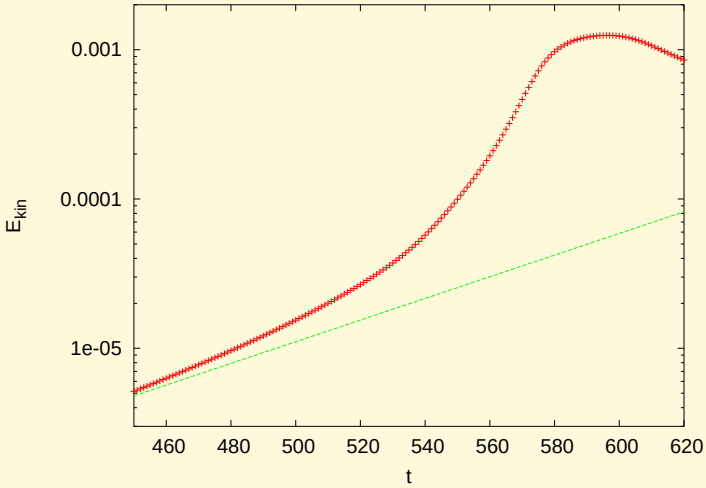

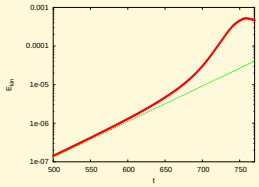

Nonlinear Hall-MHD stabilization

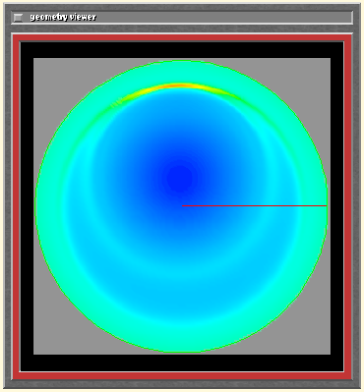

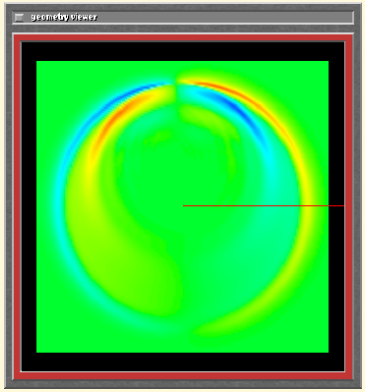

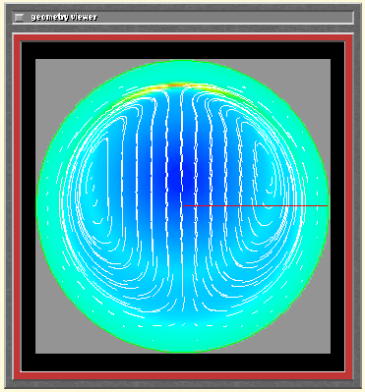

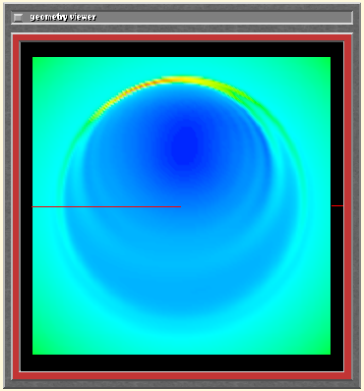

parallel current $J_{||}$

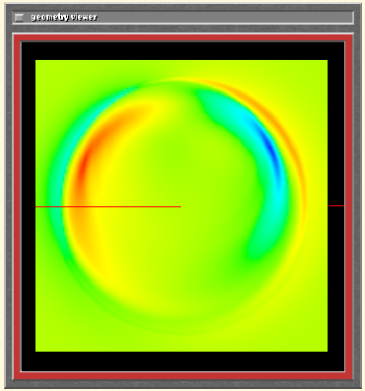

parallel vorticity

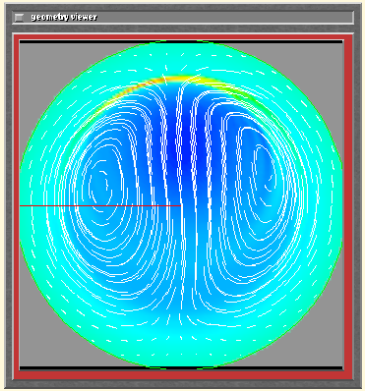

$J_{||}$ overlaid with flow

Nonlinear Hall-MHD stabilization

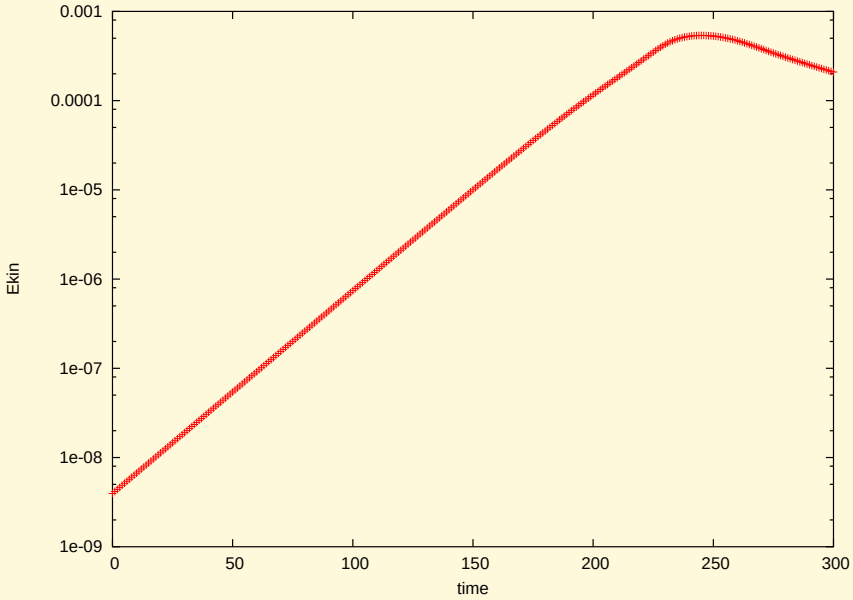

Resistive MHD: Compressible vs. Incompressible models

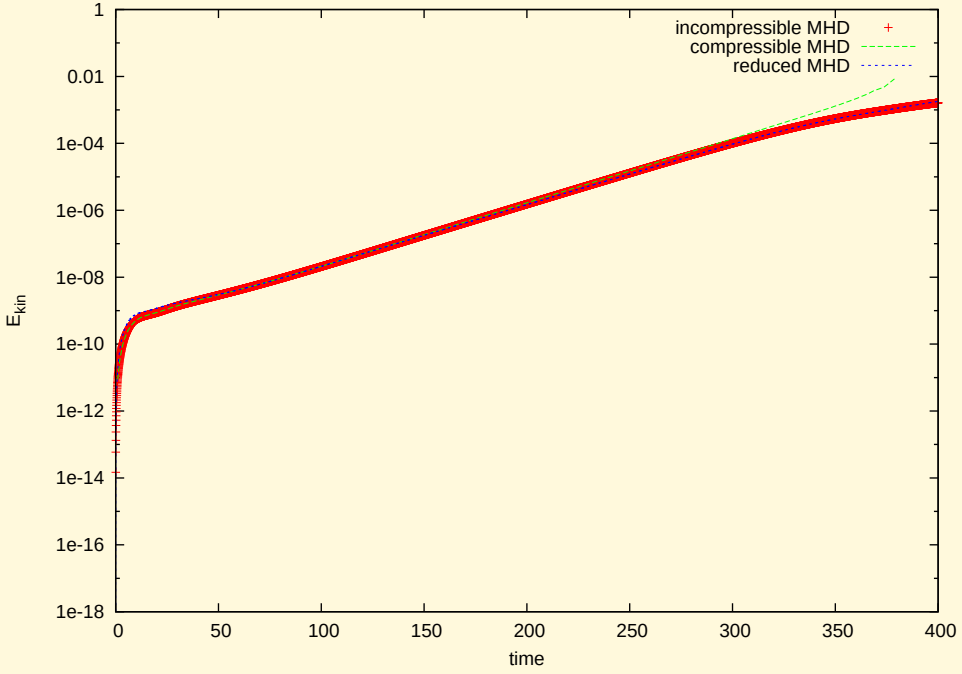

Compressible vs. incompressible evolution, linear phase:

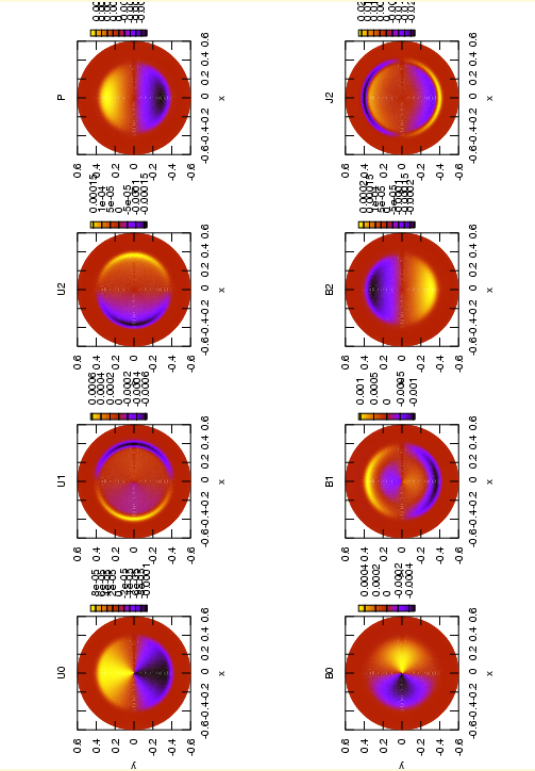

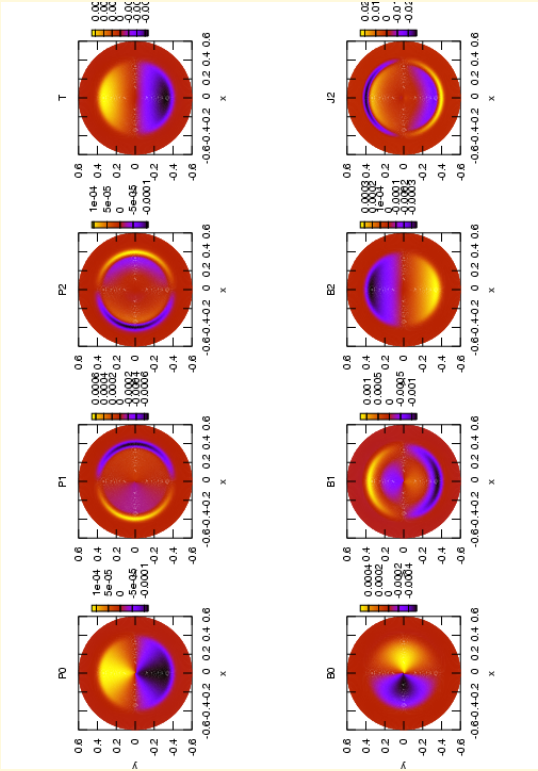

Compressible vs. incompressible evolution, nonlinear phase:

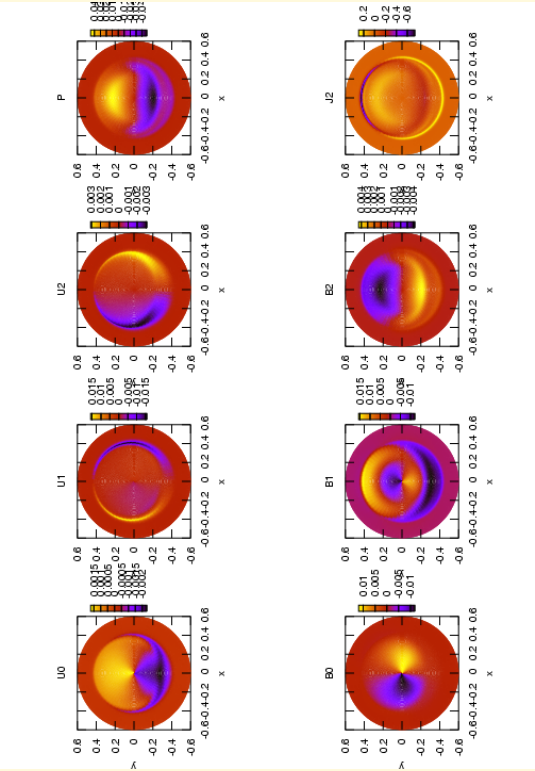

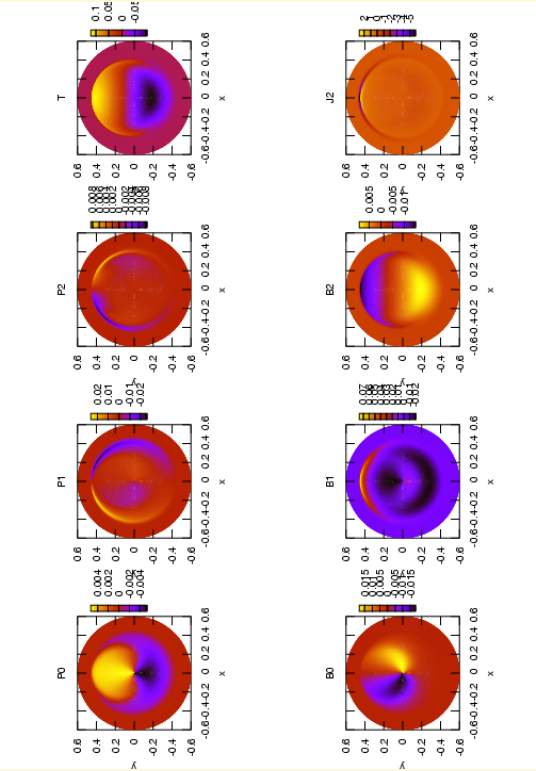

Resistive MHD: Flux pile-up

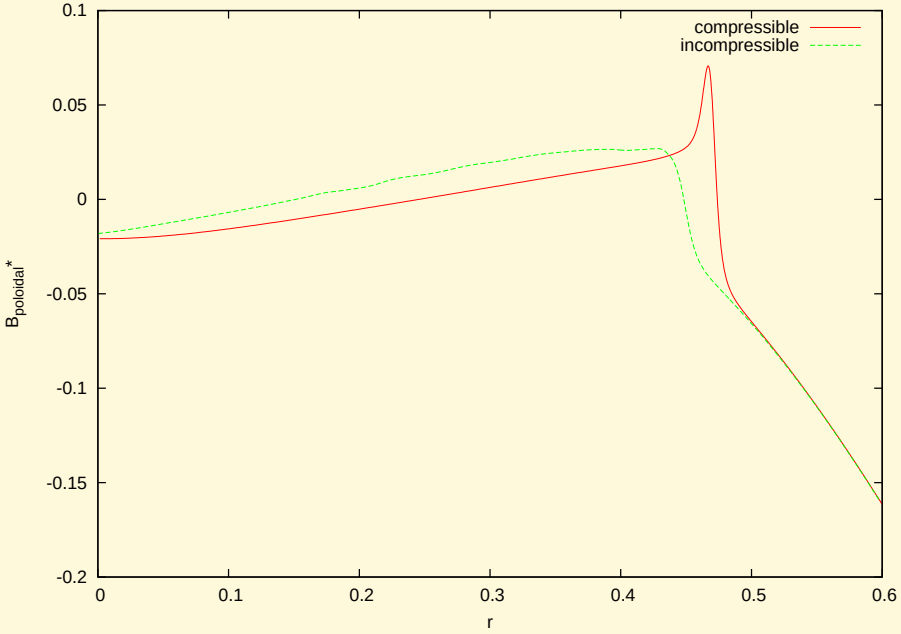

Conclusion

- Numerically exploring near-singular processes needs very high spatial and temporal resolution close to the singular time $\Longrightarrow$ AMR methods are an ideal tool.
- Implicit methods are powerful to integrate systems where the time scale of interest is much slower than that of the fastest waves.
- In 2D MHD, we clearly observed exponential growth.
- In 2D extended MHD models (Porcelli, Aydemir) we reproduced an explosive growth phase in the nonlinear evolution.
- In 3D compressible Hall-MHD, the explosive growth found in reduced models has been reproduced for certain parameters, however we also observe nonlinear stabilization in other regimes. We also find accelerated growth in compressible MHD even without two-fluid effects, whereas incompressible MHD does not show this behavior.
- More work needs to be done to gain a better understanding of the underlying reconnection physics.